



## Adaptation to Robust Monolayer Expansion Produces Human Pluripotent Stem Cells With Improved Viability

MICHAELA KUNOVA,<sup>a</sup> KAMIL MATULKA,<sup>a</sup> LIVIA EISELLEOVA,<sup>a</sup> ANTON SALYKIN,<sup>a,b</sup> IVA KUBIKOVA,<sup>a</sup> SERGIY KYRYLENKO,<sup>a</sup> ALES HAMPL,<sup>a,b</sup> PETR DVORAK<sup>a,b</sup>

**Key Words.** Embryonic stem cells • Cell culture • Xenograft assay • Cell survival • Induced pluripotent stem cells

### ABSTRACT

The generation of human pluripotent stem cells (hPSCs) of sufficient quantity and quality remains a major challenge for biomedical application. Here we present an efficient feeder-free, high-density monolayer system in which hPSCs become SSEA-3-high and gradually more viable than their feeder-dependent counterparts without changes attributed to culture adaptation. As a consequence, monolayer hPSCs possess advantages over their counterparts in embryoid body development, teratoma formation, freezing as a single-cell suspension, and colony-forming efficiency. Importantly, this monolayer culture system is reversible, preserving the competence of hPSCs to gradually reacquire features of colony growth, if necessary. Therefore, the monolayer culture system is highly suitable for long-term, large-scale propagation of hPSCs, which is necessary in drug development and pluripotent stem cell-based therapies. *STEM CELLS TRANSLATIONAL MEDICINE* 2013;2:246–254

### INTRODUCTION

The need for a robust, easy-to-handle, invariable, and cost-effective culture system for human pluripotent stem cells (hPSCs), both embryonic stem cells and induced pluripotent stem cells, is evident. For example, medical intervention after myocardial infarct requires an initial input of  $\sim 10^9$  undifferentiated hPSCs expanded in a very rapid manner to obtain a sufficient number of functional cardiomyocytes [1]. Similarly, in high-throughput drug testing, cells must be easily handled to efficiently spread over the multiwell plate [2]. Several large-scale suspension culture systems have been developed [3–5], each attempting to accommodate the embryonic nature of hPSCs that requires intense cell-cell interactions and instructive scaffolding. The main advantage of bioreactor cultures is that the environment can be precisely controlled [6]. However, the need for expensive equipment represents the main obstacle of using suspension culture systems in basic research laboratories. Therefore, the development of a robust, scalable, and easily manipulated adherent culture system for hPSCs remains an important objective.

Single-cell dissociation and plating of hPSCs in clonogenic densities has been difficult for years. Only a few studies have used fully dissoci-

ated hPSCs. These dissociated hPSCs were plated at relatively low densities, giving rise to colonies after a prolonged period of time [7–9]. The identification of Y27632, a potent inhibitor of Rho-associated protein kinase (ROCK), facilitated subcloning after gene transfer [10], enhanced the recovery of hPSCs after freezing [11], and improved reaggregation of hPSCs [12, 13]. A Y27632-independent, feeder-free, scalable method of human embryonic stem cell (hESC) propagation has been described, using full dissociation and high-density plating for the purpose of genetic modification [14]. However, the long-term sustainability of this system and the quality of cells it produces have not been tested. Herein we report a comprehensive analysis of the biological features of hPSCs after a long-term propagation as a high-density monolayer on Matrigel (BD Biosciences, Bedford, MA, <http://www.bdbiosciences.com>).

### MATERIALS AND METHODS

#### Cell Culture

Two karyotypically normal hESC lines (CCTL12 [46,XX] and CCTL14 [46,XX]) derived by ourselves and one karyotypically abnormal human induced pluripotent stem cell (hiPSC) line (hiPSC clone 4 [46,XX,der(18)t(2;18)(p13;q23), del(18)(q21.

<sup>a</sup>Department of Biology, Faculty of Medicine, Masaryk University, Brno, Czech Republic; <sup>b</sup>International Clinical Research Center, Center of Biomolecular and Cellular Engineering, St. Anne's University Hospital Brno, Brno, Czech Republic

Correspondence: Petr Dvorak, Ph.D., Department of Biology, Faculty of Medicine, Masaryk University, Kamenice 5, 625 00 Brno, Czech Republic.  
Telephone: 00420-549-491-331;  
Fax: 00420-549-491-327; E-Mail: pdvorak@med.muni.cz

Received June 27, 2012; accepted for publication December 18, 2012; first published online in *SCTM EXPRESS* March 13, 2013.

©AlphaMed Press  
1066-5099/2013/\$20.00/0

<http://dx.doi.org/10.5966/sctm.2012-0081>

1q21.3]), obtained from Dr. Majlinda Lako, Institute of Genetic Medicine, Newcastle University) were routinely maintained with irradiated (50 Gy) murine embryonic fibroblasts (mEFs) in Knock-Out Serum Replacement (KSR)-containing culture medium as described previously [15]. For the feeder-free culture of hPSCs, BD Matrigel hESC-qualified matrix (BD Biosciences) was combined with mEF-conditioned medium. For that, the KSR-containing medium was collected from the irradiated mEF culture after 24 hours for 5 days, supplemented with  $10 \text{ ng ml}^{-1}$  fibroblast growth factor-2 (FGF-2) (Peprotech, Rocky Hill, NJ, <http://www.peprotech.com>) and  $2 \text{ mmol l}^{-1}$  L-glutamine (Invitrogen, Carlsbad, CA, <http://www.invitrogen.com>) and sterile-filtered before use. To initiate the feeder-free culture, hPSC clumps were collected from the mEF-dependent culture by collagenase IV (Invitrogen) and diluted with the culture medium, and after 5 minutes of sedimentation to deplete mEFs, hPSCs located at the bottom of the tube were plated on a Matrigel-coated dish. After 5–7 days of growth as colonies, hPSCs were dissociated by TrypLE Express (Invitrogen) into a single-cell suspension and plated at high density ( $\sim 100,000 \text{ cells cm}^{-2}$ ) on a fresh Matrigel-coated dish. The cells were then passaged when approaching 100% confluence and further regularly split in a ratio to achieve confluence in 72 hours (supplemental online Fig. 1). For freezing of hPSCs, single-cell suspension was collected by TrypLE, cells were diluted with culture medium with or without  $10 \mu\text{mol l}^{-1}$  Y27632 (Sigma-Aldrich, St. Louis, MO, <http://www.sigmaaldrich.com>); mixed in a 1:1 ratio with the freezing solution containing 20% dimethylsulfoxide, 60% ES-Cell Qualified Fetal Bovine Serum (Invitrogen), and 20% culture medium; and stored in liquid nitrogen.

### Immunocytochemistry

Cells were fixed with 4% (wt/vol) paraformaldehyde at room temperature for 5 minutes followed by methanol treatment at  $-20^\circ\text{C}$  for 5 minutes. Immunostaining was performed as described previously [15]. The primary antibodies were as follows: mouse monoclonal to Oct-4 (sc-5279; Santa Cruz Biotechnology, Santa Cruz, CA, <http://www.scbt.com>), rabbit polyclonal to Nanog (sc-33759; Santa Cruz Biotechnology), rabbit monoclonal to Sox2 (3579; Cell Signaling Technology, Danvers, MA, <http://www.cellsignal.com>), mouse monoclonal to SSEA-4 (MAB4304; Chemicon, Billerica, MA, <http://www.chemicon.com>), mouse monoclonal to TRA-1-60 (MAB4360; Chemicon), goat polyclonal to Gata6 (sc-7244; Santa Cruz Biotechnology), mouse monoclonal to AFP (18-0003; Invitrogen), and mouse monoclonal to Pax6 (Developmental Studies Hybridoma Bank, Iowa City, IA, <http://www.uiowa.edu/~dshbwww>). Microscopic analysis was performed using the Olympus Cell<sup>^</sup>R Imaging Station (Olympus, Prague, Czech Republic, <http://www.olympus-global.com>) or FluoView 500 laser scanning microscope (Olympus). Images were processed using Adobe Photoshop software (Adobe Systems Inc., San Jose, CA, <http://www.adobe.com>).

### Flow Cytometry

To analyze the expression of surface markers by flow cytometry, hPSCs were harvested and processed as described previously [15]. The following primary antibodies provided by Dr. Peter W. Andrews (Department of Biomedical Science, University of Sheffield) were used to detect cell surface antigen expression: rat monoclonal to SSEA-3 and mouse monoclonal to TRA-1-81. The antibody specific for SSEA-5 was purchased from Abcam (ab3355; Cambridge, U.K., <http://www.abcam.com/>).

Flow cytometry was performed using a Cytomics FC500 cytometer (Beckman Coulter, Fullerton, CA, <https://http://www.beckmancoulter.com>). Analysis was done with FlowJo software (Tree Star, Ashland, OR, <http://www.treestar.com>).

### Semiquantitative Reverse Transcription-Polymerase Chain Reaction (RT-PCR) and Quantitative Real-Time RT-PCR

Total RNA was isolated using RNA Blue reagent (Top-Bio, Prague, Czech Republic, <http://www.top-bio.cz>) according to the manufacturer's instructions. For semiquantitative RT-PCR, cDNA was synthesized by Moloney murine leukemia virus reverse transcriptase (Invitrogen) at  $37^\circ\text{C}$  for 1 hour followed by 15 minutes at  $65^\circ\text{C}$ . The PCR profiles and primer sequences (Generi-Biotech, Hradec Kralove, Czech Republic, <http://www.generi-biotech.com>) were as described previously [15]. For quantitative real-time RT-PCR, cDNA was synthesized by Transcriptor first strand cDNA synthesis kit (Roche, Mannheim, Germany, <https://www.roche-applied-science.com>). PCR conditions as well as TaqMan Gene Expression Assays for *NANOG*, *TGDF1*, *GABRB3*, *DNMT3B*, *GDF3*, *POU5F1*, *GAPDH*, and *BCL2L1* (Hs00236329\_m1; specifically targeting mRNA for the Bcl-xL protein, but not Bcl-xS) (all from Applied Biosystems, Foster City, CA, <http://www.appliedbiosystems.com>) were used as described previously [15]. DNA amplification was detected using a LightCycler 480 II (Roche). Relative mRNA levels were normalized to GAPDH.

### Colony-Forming and Plating Efficiency Assays

To determine colony-forming efficiency, hPSCs were dissociated with TrypLE into single-cell suspensions and plated into 24-well plates at different concentrations ( $100\text{--}10,000 \text{ cells cm}^{-2}$ ), and the one with the highest ratio of colonies to number of plated cells (always the lowest plating density giving rise to colonies—usually  $10\text{--}30 \text{ colonies cm}^{-2}$ ) was used to calculate colony-forming efficiency. To test attachment and growth of hPSCs in colonies (plating efficiency), uniform hPSC clumps were generated using the STEMPRO EZPassage tool (Invitrogen) and plated into 24-well plates. For both assays, cells were fixed with 4% paraformaldehyde at room temperature for 15 minutes and stained with 0.05% (wt/vol) crystal violet in deionized water 5–7 days after plating. The efficiency was determined by manual counting of colonies.

### Differentiation of hPSCs

For in vitro differentiation of hPSCs, embryoid bodies as well as adherent outgrowths of hPSCs were prepared as described previously [15]. In vivo differentiation capacity of hESCs was examined by teratoma formation assay. All animal studies were carried out following approved guidelines (project no. 02/2010). For the teratoma assay, uniform clumps of hESCs were prepared using the STEMPRO EZPassage tool. An inoculum of  $1 \times 10^6$  cells (if not indicated otherwise) in  $100 \mu\text{l}$  of culture medium was injected into the hind limb muscle of 6–8-week-old NOD/SCID/IL2Rg-null mice. When tumor diameters reached  $\sim 1 \text{ cm}$ , mice were euthanized by cervical dislocation. Tumors were gently dissected from surrounding tissue and fixed in Bouin's solution for 24 hours followed by 72 hours in 5% (wt/vol) formalin. After dehydration (ethanol), brightening (cedar oil), and soaking (paraffin), the tissue was embedded in Paraplast (Sigma-Aldrich) and sectioned ( $5 \mu\text{m}$ ). Sections were stained with hematoxylin and eosin to visualize tissue structure. To counterstain the cartilage

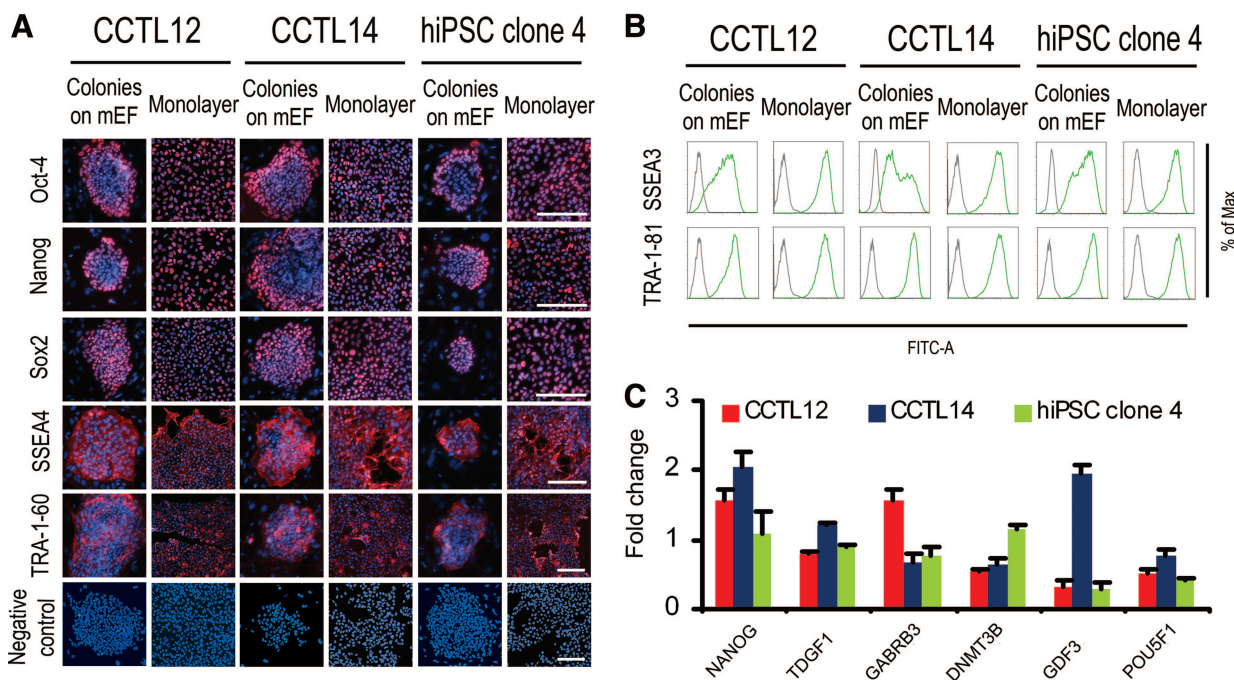


**Figure 1.** Expression of human pluripotent stem cell (hPSC) markers in both human embryonic stem cells and hiPSCs grown either as a monolayer or in colonies on mEFs. **(A):** Immunodetection of Oct-4, Nanog, Sox2, SSEA-4, and TRA-1-60. Negative control used a standard workflow, but without primary antibody. Scale bars = 100  $\mu$ m. **(B):** Representative flow cytometric results for surface markers TRA-1-81 and SSEA-3 (green lines). Gray lines show isotype controls. **(C):** Quantitative reverse transcription-polymerase chain reaction for *NANOG*, *TDGF1*, *GABRB3*, *DNMT3B*, *GDF3*, and *POU5F1* normalized to *GAPDH*. The columns show fold change of gene expression in monolayer hPSCs relative to colonies on mEFs. Error bars indicate SEM ( $n = 3$ ). Abbreviations: FITC, fluorescein isothiocyanate; hiPSC, human induced pluripotent stem cell; Max, maximum; mEF, murine embryonic fibroblast.

and/or goblet cells, Alcian blue was used to stain the mucopolysaccharides and glycosaminoglycans. For the 7-day adherent differentiation of hPSCs, cells were daily treated with 5  $\mu$ mol l<sup>-1</sup> all-trans-retinoic acid (Sigma-Aldrich).

### Karyotype Analysis

Cells in metaphase were collected as previously described [15] and kindly analyzed by Dr. Duncan Baker (Sheffield Diagnostic Genetic Services, Centre for Stem Cell Biology, University of Sheffield).

### Western Blot Analysis

Cells were washed with phosphate-buffered saline and lysed in 100 mmol l<sup>-1</sup> Tris-HCl (pH 6.8) containing 20% glycerol and 1% sodium dodecyl sulfate (SDS). Protein concentrations were determined using the DC Protein Assay Kit (Bio-Rad, Hercules, CA, <http://www.bio-rad.com>). Lysates with equal protein concentrations were supplemented with 0.01% bromophenol blue and 1%  $\beta$ -mercaptoethanol and boiled for 10 minutes. Equal amounts of total protein were separated by SDS-polyacrylamide gel electrophoresis and electrotransferred onto Immobilon-P polyvinylidene difluoride membrane (Millipore, Billerica, MA, <http://www.millipore.com>). Membranes were then blocked with 5% low-fat milk and incubated with primary and the appropriate secondary antibody. Primary antibodies were as follows: mouse monoclonal to  $\alpha$ -tubulin (11-250-C100; EXBIO Praha, Vestec, Czech Republic, <http://www.exbio.cz>), rabbit monoclonal to Oct-4 (sc-5279; Santa Cruz Biotechnology), rabbit monoclonal to survivin (2808; Cell Signaling Technology), rabbit monoclonal to Bcl-xL (2764; Cell Signaling Technology), and rabbit monoclonal to Bcl-2 (4223; Cell Signaling Technology). Protein

bands were visualized using the ECL Plus reagent (Amersham Biosciences, Little Chalfont, U.K., <http://www.amersham.com>).

### Statistical Analysis

Throughout the text, data were reported as mean  $\pm$  SEM. For statistical significance, the two-tailed Student's *t* test was used whenever the data met the criteria. Paired tests were used in experimental setups using cells arising from the same pool, that is, in Y27632 treatment-based in vitro experiments. In teratoma experiments, the statistics were calculated by two-sample binomial test with continuity correction. The significance  $\alpha = 0.05$  level was used for all analyses.

## RESULTS

The monolayer culture system presented here is based on single-cell dissociation and cell plating at high densities on a Matrigel-coated surface, so that cells become fully confluent within 72 hours (Materials and Methods; supplemental online Fig. 1). Probing of monolayer hPSCs for markers of pluripotency revealed minor differences compared with the colony-based feeder-dependent culture (Fig. 1). Whereas colonies grown with mEFs developed the previously described [16] edge-to-center gradient of Oct-4 and Nanog, this expression pattern in the monolayer system was random (Fig. 1A). Flow cytometry showed that hPSCs grown as mEF-dependent colonies contain SSEA-3-low and -high subpopulations, but this heterogeneity was absent in monolayer hPSCs, in which only a single SSEA-3-high population was found (Fig. 1B). Quantitative RT-PCR for a larger panel of hPSC marker genes revealed no substantial

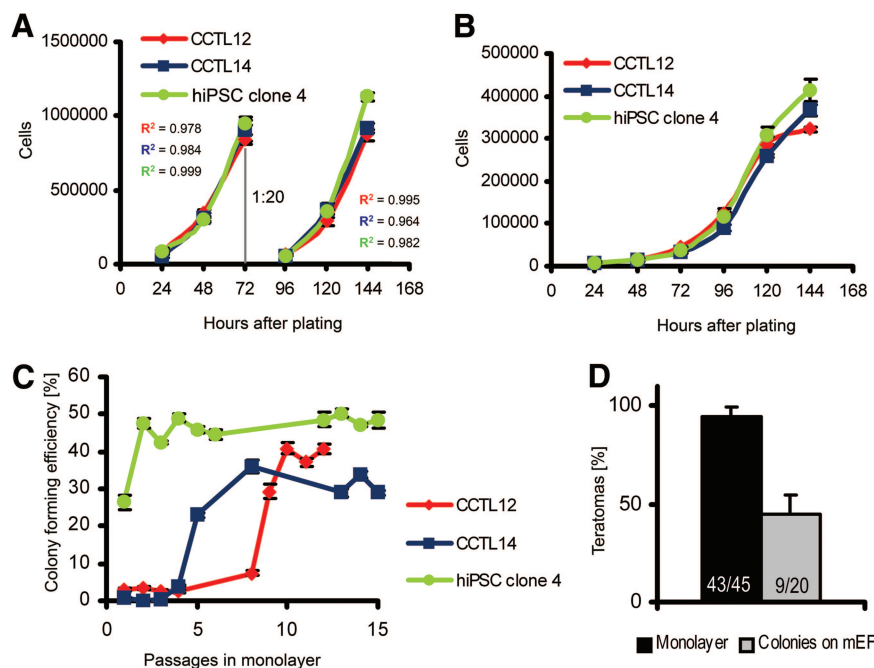


**Figure 2.** Human pluripotent stem cell (hPSC) growth in feeder-free monolayer culture and in colonies on mEFs. **(A):** Growth kinetics of hPSCs in monolayer culture. Splitting of cells, performed at a 1:20 ratio after 72 hours of culture, is indicated.  $R^2$  (coefficient of determination) indicates the plausibility of exponential growth. Error bars indicate SEM ( $n = 5$ ). **(B):** Growth kinetics of hPSCs in mEF-dependent colony culture. Error bars indicate SEM ( $n = 5$ ). **(C):** Colony-forming efficiency of hPSCs during the initial 15 passages in monolayer culture. Error bars indicate SEM ( $n = 6$ ). **(D):** Teratoma-forming efficiency of human embryonic stem cells (hESCs) in monolayer culture or in colonies on mEFs. Data were generated from CCTL12 and CCTL14 cells. The numbers in the columns show the number of mice that developed teratomas compared with the total number of mice that received intramuscular injections of hESCs. Error bars indicate SEM. Abbreviations: hiPSC, human induced pluripotent stem cell; mEF, murine embryonic fibroblast.

and/or reproducibly present differences between mEF-dependent and feeder-free monolayer cultured hPSCs (Fig. 1C). Observed differences might reflect reaction of monolayer hPSCs to an environment lacking spatial inhibition and direct stimulation by mEFs, which generates microdomains with Oct-4 and Nanog gradients [17]. However, the gradients could also be affected by the short splitting interval and exponential growth, which persists between plating and splitting in the monolayer system (Fig. 2A), in contrast to the long lag-phase in colony-based growth (Fig. 2B). Monolayer culture resulted in efficient expansion, with the colony-forming efficiency of hPSCs gradually increasing to  $38.4 \pm 2.3\%$  after 10 passages in monolayer (Fig. 2C). Consequently, it allowed for a splitting ratio of 1:20 with a 3-day splitting interval. This produced a clinically relevant population of  $2.5 \times 10^{10}$  hPSCs in 4 weeks (supplemental online Fig. 2).

Selection of particular hPSCs during culture, which might lead to clonal expansion and changes in hPSC phenotype, including their ability to differentiate or proliferate, remains a critical issue when culture conditions are altered. Therefore, we first compared the differentiation capacity of hPSCs cultured in monolayer and in mEF-dependent colonies by embryoid body (EB) formation, EB formation combined with adherent growth, and in hESCs also by a xeno-grafting teratoma assay. The results showed virtually identical capacities of hPSCs from both culture systems to form derivatives of all three germ layers *in vitro* (supplemental online Fig. 3a, 3b) and by hESCs also *in vivo* (supplemental online Fig. 3c), which is consistent with our previous observation [15]. However, the teratoma formation assay revealed that hESCs adapted in monolayer culture produced teratomas in  $94.3 \pm 4.9\%$  of cases when  $1 \times 10^6$  hESCs were injected, whereas

cells grown in mEF-dependent colonies showed a lower efficiency of  $45.0 \pm 9.6\%$  ( $p < .001$ , two-sample binomial test; Fig. 2D). Notably, the increased teratoma-forming efficiency is not attributable to growth in the presence of Matrigel, as hESC colonies grown without mEFs on Matrigel formed no teratomas in 11 mice injected. Therefore, hPSCs in both monolayer and colonies are capable of comparable multilineage differentiation, but monolayer hESCs better form teratomas.

We further tested whether the monolayer system triggers selection and clonal expansion of hPSCs. This is conceivable, as the first passages in the monolayer system are accompanied by increased cell death, presumably a consequence of single-cell dissociation of hPSCs. Dissociation-induced apoptosis of hESCs can be blocked using Y27632 [18]. Therefore, we used Y27632 during plating in three initial passages in monolayer culture, thus reducing potential selective pressure based on superior attachment or survival after cell dissociation. However, we obtained hESCs with similarly high teratoma-forming efficiency as from cultures without Y27632, indicating a nonselective process of adaptation to monolayer culture. This is further supported by the lack of karyotypic changes in hPSCs during monolayer culture (supplemental online Fig. 4).

To determine the minimal number of hESCs required to form teratomas, we injected decreasing numbers of cells into mice. Interestingly, at  $1.0 \times 10^5$  and  $1.0 \times 10^4$  cells, we observed comparable decreases of teratoma-forming efficiency in both groups of hESCs, always accompanied by prolonged latency (Fig. 3A). However, when the number of injected cells maintained in colonies was increased from  $1.0 \times 10^6$  to  $5.0 \times 10^6$ , teratoma-forming capacity increased from  $50.0 \pm 10.0\%$  to  $90.0 \pm 10.0\%$

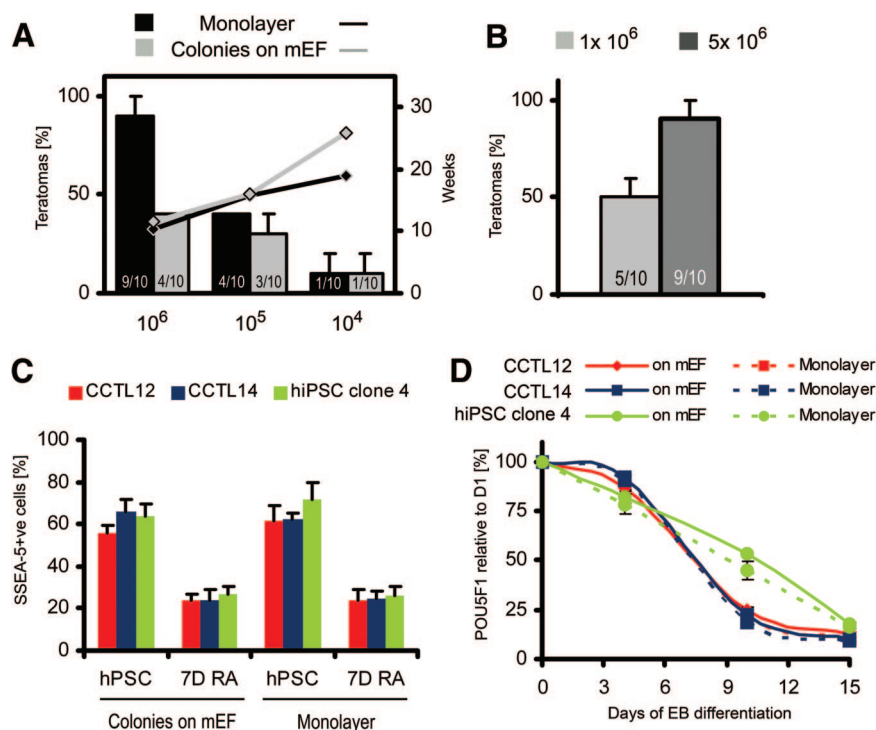


**Figure 3.** Teratoma-forming efficiency of human embryonic stem cells (hESCs). **(A):** Teratoma-forming efficiency (columns) and average latency (lines) of teratoma development after injection of decreasing number of hESCs. Data were generated from CCTL12 and CCTL14 cells. The numbers in the columns show the number of mice that developed teratomas compared with the total number of mice that received intramuscular injections of hESCs. Error bars indicate SEM. **(B):** Teratoma-forming efficiency of mEF-dependent colonies after injection of standard ( $1 \times 10^6$ ) or increased ( $5 \times 10^6$ ) numbers of hESCs from the CCTL12 and CCTL14 lines. The numbers in the columns show number of mice that developed teratomas compared with the total number of mice that received intramuscular injections of hESCs. Error bars indicate SEM. **(C):** Flow cytometric analysis showing the percentage of SSEA-5-positive cells in undifferentiated hPSCs and in cells treated with  $5 \mu\text{mol l}^{-1}$  all-trans-retinoic acid for 7 days. Error bars indicate SEM ( $n = 4$ ). **(D):** Quantitative reverse transcription-polymerase chain reaction for *POU5F1* transcript levels normalized to *GAPDH* during 15-day EB differentiation. Error bars indicate SEM ( $n = 3$ ). Abbreviations: +ve, positive; 7D RA, treatment with all-trans-retinoic acid for 7 days; hiPSC, human induced pluripotent stem cell; hPSC, human pluripotent stem cell; mEF, murine embryonic fibroblast.

( $p = .0189$ , two-sample binomial test; Fig. 3B), a level comparable with monolayer hESCs. Thus, in accordance with the teratoma frequency shown in Figure 2D, the threshold number of hESCs necessary to develop a teratoma is within the range of  $1.0\text{--}5.0 \times 10^6$  for mEF-dependent hESCs and  $0.1\text{--}1.0 \times 10^6$  for monolayer hESCs, indicating either different proportions of teratoma-initiating cells or distinct survival rates early after injection.

Recently, surface glycan SSEA-5 was shown to specifically mark teratoma-initiating hPSCs [19]. During differentiation, SSEA-5 is depleted from the cell surface; consequently, cells lose teratoma-forming capacity. Thus, we asked whether an increased pool of SSEA-5-positive cells increases teratoma-forming capacity in monolayer hESCs. We examined SSEA-5 expression in undifferentiated and differentiating hPSCs from both culture systems. Virtually the same level of SSEA-5 positivity was observed within undifferentiated cells or within cells after 7 days of differentiation (Fig. 3C; supplemental online Fig. 5). In addition, *POU5F1* (encoding Oct-4 protein) expression did not differ after 15 days of EB differentiation between monolayer hPSCs and colonies (Fig. 3D). hiPSC clone 4 cells showed a distinct dynamics of differentiation; however, the invariance between colonies and monolayer was preserved. Therefore, teratomas developed from monolayer hESCs were likely not driven by an increased pool of teratoma-initiating and/or differentiation-resistant cells.

Cell death also influences teratoma development, as significant numbers of hPSCs die shortly after injection [20]. Thus, cell populations with increased resistance to cell death would more efficiently form teratomas. Recently, the effects of antiapoptotic proteins Bcl-2 and Bcl-xL on hESC survival were described [21–23]. In addition, survivin has been shown to regulate hESC teratoma-forming capacity [24]. However, none of these factors were overexpressed in monolayer hPSCs compared with colonies (Fig. 4). Of note, the expression of survivin was remarkably low in CCTL14 colonies growing on Matrigel (Fig. 4A), which correlates with no teratomas developed out of these cells.

To investigate further whether the increased viability of monolayer cells resulted in increased teratoma-forming capacity, we evaluated the plating efficiency of cells after preparation for injection (described in Materials and Methods). The plating efficiency, which combines cell viability and attachment, decreased significantly more in hESC colonies on mEFs than in monolayer hESCs after 120 minutes (Fig. 5A), specifically by  $65.8 \pm 4.8\%$  and  $40.2 \pm 2.0\%$  in CCTL12 clumps from monolayer and mEF-dependent colonies, respectively ( $p = .005$ ,  $t$  test), and by  $62.1 \pm 5.9\%$  and  $33.8 \pm 6.7\%$  in CCTL14 clumps from monolayer and mEF-dependent colonies, respectively ( $p = .01$ ,  $t$  test). When hESC clumps were incubated with Y27632, the difference between the samples was eliminated (Fig. 5A). There was no significant effect of Y27632

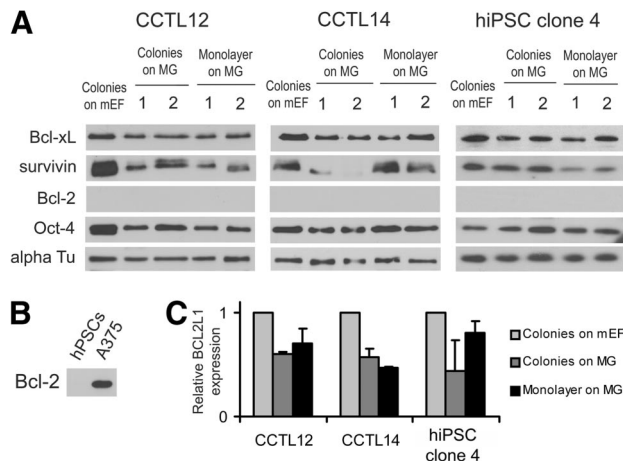


**Figure 4.** Expression of hPSC survival-associated antiapoptotic genes in the monolayer system, colonies on MG, and standard culture in colonies on mEFs. **(A):** Western blot for Bcl-xL, survivin, and Bcl-2 in hPSCs cultured in colonies on mEFs, colonies on MG, or as a monolayer on MG. Note that Bcl-2 was not detected. Numbers indicate independent samples. Oct-4 served as a marker of the undifferentiated state of hPSCs;  $\alpha$ -tubulin served as a loading control. **(B):** A375, a melanoma cell line, served as a positive control for the anti-Bcl-2 antibody in the Western blot. **(C):** Quantitative reverse transcription-polymerase chain reaction for the *BCL2L1* gene (encoding Bcl-xL protein) normalized to *GAPDH*. The results indicate higher expression of *BCL2L1* in colonies on mEFs, which is also visible by Western blot **(A)**. Error bars indicate SEM ( $n = 6$ ). Abbreviations: alpha Tu,  $\alpha$ -tubulin; hPSC, human pluripotent stem cell; mEF, murine embryonic fibroblast; MG, Matrigel.

on the plating efficiency of hiPSC clone 4 cells, neither growing in colonies on mEFs nor in the monolayer system (Fig. 5A). These results suggest that differences between monolayer hPSCs and mEF-dependent colonies involve cell survival.

We also observed increased yields of EBs in monolayer hPSCs versus colonies on mEFs. Therefore, we performed EB formation assay in which Y27632 was present or absent during the aggregation step. Without Y27632, strikingly poor aggregation followed by progressive cell death in colony-related samples (supplemental online Fig. 6) led to lower EB yields than monolayer-derived EBs (Fig. 5B), specifically  $1.7 \pm 0.2$ -fold in CCTL12 hESCs ( $p = .003$ ,  $t$  test),  $3.0 \pm 0.6$ -fold in CCTL14 hESCs ( $p < .001$ ,  $t$  test), and  $1.4 \pm 0.2$ -fold in hiPSC clone 4 cells ( $p = .001$ ,  $t$  test). Supplementation of Y27632 during aggregation improved the yields of colony-derived EBs (Fig. 5B), specifically  $1.6 \pm 0.1$ -fold in CCTL12 hESCs ( $p = .006$ , paired  $t$  test),  $2.2 \pm 0.4$ -fold in CCTL14 hESCs ( $p < .001$ , paired  $t$  test), and  $1.5 \pm 0.1$ -fold in hiPSC clone 4 cells ( $p < .001$ , paired  $t$  test). However, the beneficial effect of Y27632 was weaker for monolayer-derived EBs yields (Fig. 5B), with only  $1.3 \pm 0.1$ -fold increased yields in CCTL12 hESCs ( $p = .008$ , paired  $t$  test),  $1.2 \pm 0.2$ -fold increased yields in CCTL14 hESCs ( $p = .02$ , paired  $t$  test), and  $1.2 \pm 0.2$ -fold increased yields in hiPSC clone 4 cells ( $p = .01$ , paired  $t$  test).

Y27632 can also improve the recovery of hPSCs after thawing [11]. We showed that Y27632 supplementation during post-thaw plating increased the colony-forming efficiency of mEF-dependent colonies  $3.5 \pm 0.6$ -fold ( $p = .001$ , paired  $t$  test) and  $2.8 \pm 0.4$ -fold ( $p = .002$ , paired  $t$  test) in CCTL12 and CCTL14 hESCs, respectively (Fig. 5C). However, Y27632 increased the post-thaw colony-forming efficiency of monolayer hESCs only  $1.4 \pm 0.1$ -fold ( $p = .01$ , paired  $t$  test) and  $1.3 \pm 0.1$ -fold ( $p = .007$ , paired  $t$  test) in CCTL12 and CCTL14

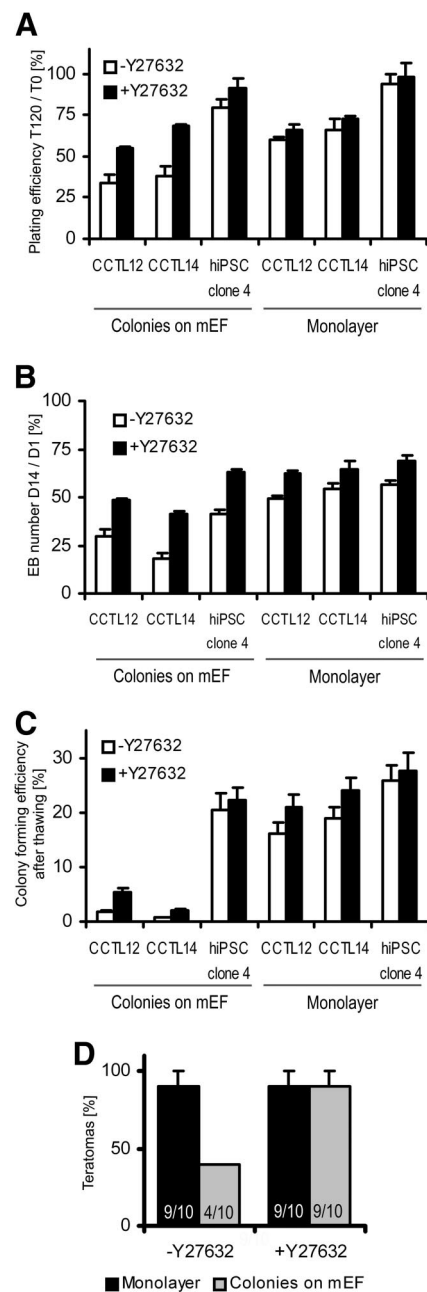


**Figure 5.** Functional assays of human pluripotent stem cell (hPSC) viability. **(A):** Plating efficiency of hPSC clumps after 120 minutes in suspension. Cell clumps were processed either without or with Y27632. Error bars indicate SEM ( $n = 6$ ). **(B):** The yields of differentiating EBs that were aggregated in AggreWell plates from hPSC suspension either without or with Y27632. Error bars indicate SEM ( $n = 5$ ). **(C):** Effect of Y27632 on post-thawing colony-forming efficiency of hPSCs frozen as a single-cell suspension. Error bars indicate SEM ( $n = 6$ ). **(D):** Effect of Y27632 on teratoma-forming efficiency of CCTL12 and CCTL14 cells grown as colonies on feeders or in monolayer culture. The numbers in the columns show the number of mice that developed teratomas compared with the total number of mice that received intramuscular injections of human embryonic stem cells. Error bars indicate SEM. Abbreviations: hiPSC, human induced pluripotent stem cell; mEF, murine embryonic fibroblast.

cells, respectively (Fig. 5C). There was no significant effect of Y27632 on the colony-forming efficiency of hiPSC clone 4 cells, neither growing in colonies on mEFs nor in the monolayer system (Fig. 5C).

**Table 1.** Teratoma-forming efficiency of CCTL14 hESCs

	Colonies on mEFs	ML2	ML10	REV p1	REV p5
–Y27632	40% (2/5)	0% (0/5)	80% (4/5)	80% (4/5)	40% (2/5)
+Y27632	80% (4/5)	20% (1/5)	80% (4/5)	Not tested	100% (5/5)

Table shows the teratoma-forming efficiency of CCTL14 hESCs grown in colonies with mEFs, early (ML2) and adapted (ML10) monolayer culture, and early (REV p1) and late (REV p5) reverted colonies on mEFs. The cells were treated with Y27632 or left untreated before injection into recipient mice. The numbers in parentheses show the number of mice that developed teratomas compared with the total number of mice that received intramuscular injections of hESCs.

Abbreviations: hESC, human embryonic stem cell; mEF, murine embryonic fibroblast.

We conclude that although Y27632 significantly promotes survival of mEF-dependent hESCs subjected to various stresses, it has only a minor effect on monolayer hESCs. To determine whether the same effect could be seen *in vivo*, we injected hESCs into mice with or without Y27632. The presence of Y27632 in the hESC inoculum significantly improved the teratoma-forming efficiency of hESC colonies toward the level exhibited by monolayer hESCs ( $p = .006$ , two-sample binomial test; Fig. 5D).

Finally, we examined whether the monolayer system produces hPSCs with an irreversibly changed phenotype. CCTL14 hESCs maintained for at least 35 passages in monolayer culture could be reverted back to colony growth (supplemental online Fig. 7a–7c), with morphology and pluripotency marker gradients of Oct-4 and Nanog identical to those of hESCs maintained exclusively in colonies. These monolayer-reverted mEF-dependent hESCs gradually regained low teratoma-forming efficiency (Table 1) and dependence on Y27632 *in vitro* (supplemental online Fig. 7d, 7e) and *in vivo* (Table 1), characteristics of mEF-dependent colonies. These results further demonstrate the absence of irreversible selection in the monolayer system.

## DISCUSSION

It had been thought that hPSCs could not be successfully propagated for a prolonged time following single-cell dissociation, which was attributed to the extremely low clonogenic capacity of hPSCs [25] and early onset of chromosomal abnormalities [7]. However, it is the strict requirement of cell-cell contact that leads to cell death when hPSCs are plated in densities prohibiting cell clustering [26, 27]. By overexpressing the antiapoptotic protein Bcl-2 [21] or Bcl-xL [23], hESCs become more resistant to cell death. In the high-density monolayer culture system presented in this study, hPSCs gradually acquired a high colony-forming efficiency. Nevertheless, we did not observe elevated levels of Bcl-2 or Bcl-xL in these cells. Rapid increases in hESC clonogenicity have previously been shown to be coupled to the onset of chromosomal abnormalities [7]. Although minor genomic alterations that can develop in hESC culture [28] were not tested in our study, we have never observed any change in karyotype during propagation of hPSCs. This is presumably a consequence of the high plating and growth densities, which in turn eliminates cell death linked to dissociation through the rapid formation of hPSC clusters. Thus, no substantial cell death occurs, and hPSCs are under no considerable selective pressure.

Generally, all the cell lines and sublines can adapt to the monolayer culture. However, there is a variability in time required for adaptation, as some lines adjust easily (within 1–2 passages in the monolayer system; e.g., hiPSC clone 4 cells, where it is presumably caused by the chromosomal abnormality), but for some other hPSC lines, it takes a longer time. In

karyotypically normal cells (as represented by CCTL12 and CCTL14 hESCs), there is an adaptation interval of 3–5 passages, where the colony-forming and plating efficiencies are very low, so the splitting ratio used to preserve the 3-day splitting interval needs to be 1:3 to 1:5. After that, always within an interval of next 2–3 passages, the cells quickly enhance their colony-forming efficiencies and keep these very high for a prolonged time (more than 100 passages tested in CCTL14 hESCs). These cells are “adapted” to the monolayer culture and can be propagated using a 1:20 ratio every 3 days.

Within an hESC colony, SSEA-3-high, -low, and -negative cells can be identified [29]. Although these populations are interconvertible, they possess distinct immediate properties. For example, it is the SSEA-3-high subpopulation that is highly clonogenic [29–31]. In our study, we observed a pronounced homogenization of monolayer hPSCs with a shift to high levels of SSEA-3 expression. This feature can therefore contribute to the increased clonogenic capacity of monolayer hPSCs. As the homogeneously high levels of SSEA-3 remain to be present also in monolayer cells directly after thawing (supplemental online Fig. 8), this might lead to better post-thawing colony-forming efficiency of monolayer hPSCs.

Globo-series glycosphingolipids, such as SSEA-3, have a significant role in aggregation of cells [32]. Therefore, high levels of SSEA-3 can lead to better aggregation of monolayer hPSCs, which in turn causes superior yields of EBs, as the aggregation is a crucial step using the AggreWell (StemCell Technologies, Vancouver, BC, Canada, <http://www.stemcell.com>) technique of EB formation. Presumably, high levels of SSEA-3 also increase aggregation of monolayer hESCs early after injection into the animal host during teratoma formation assay, by this enhancing the efficiency of teratoma formation. As a consequence, fewer monolayer hESCs were required to successfully develop a teratoma relative to the colony-based hESCs.

Y27632 was identified as a potent regulator of dissociation-induced cell death of hESCs [10]. We observed that hPSCs propagated in monolayer respond to Y27632 treatment only minimally. However, these hPSCs were functionally superior to hPSC colonies. It is therefore likely that monolayer hPSCs have reached maximal resistance to dissociation-induced cell death solely by intrinsic mechanisms. The high plating density may have allowed for fast cell clustering and stabilization of E-cadherin on the cell surface of monolayer hPSCs, a process promoting hPSC survival after single-cell dissociation [26, 27, 33].

Of note, high-density monolayer hPSCs are temporally resistant to suboptimal culture. They could be propagated in unconditioned medium or without any recombinant FGF-2 for at least five passages. After that, their growth rate slowed, but they did not undergo any significant differentiation as observed in hPSC colonies cultured in suboptimal conditions (data not shown). It has been noted that resistance to withdrawal of extrinsic stimuli

is associated with “variant” hESCs, those of usually abnormal karyotype, exceptional cell survival, and efficient propagation [34]. However, when monolayer hPSCs were grown back as low-density colonies, they immediately became sensitive to deficient culture medium, which was followed by extensive differentiation and/or cell death. This suggests that monolayer hPSCs are not variant and that they can be readily reverted to colony growth, if necessary. This conversion is also accompanied by the re-establishment of other features of colony growth: an edge-to-center gradient of Nanog and Oct-4, responsiveness to Y27632, and poorer function, particularly EB and teratoma formation.

In our study, we used mEF-conditioned KSR-based culture medium and Matrigel matrix to propagate high-density feeder-free monolayer hPSCs. These are obviously neither xeno-free nor defined components of the culture environment. For efficient drug development and safe pluripotent stem cell-based therapies, however, the culture of hPSCs must be simple, defined, and animal protein-free. We have shown that monolayer hESCs can be propagated in completely defined, serum-free, and animal protein-free medium containing plant hydrolysate VegetaCell (Chemispol, Kutna Hora, Czech Republic) [15]. Also, commercially available defined mTeSR1 medium can be used to propagate monolayer hESCs for at least 20 passages without any change in performance or marker expression (data not shown). Additionally, completely xeno-free culture conditions, including recombinant laminin-511 and xeno-free culture media, have been shown to also be compatible with high-density feeder-free growth of hPSCs [35]. This indicates that feeder-free high-density monolayer culture is a universal culture system for hPSCs.

## CONCLUSION

We showed that feeder-free monolayer culture is a robust and efficient method for large-scale propagation of hPSCs. We did not find any discriminating features between cells from each culture system, except for higher viability, which is not linked to the upregulation of antiapoptotic genes previously associated with hPSC survival. In the monolayer system, hPSCs became ho-

mogenized and SSEA-3-high. Thus, monolayer hPSCs are extremely useful for use in assays involving dissociation, such as cell sorting, transfection, and subcloning. Importantly, the monolayer system is fully reversible: monolayer hPSCs may be grown as colonies and adopt all features associated with colony growth. Simple automation and compatibility with xeno-free conditions make the monolayer system highly suitable for the production of the vast numbers of hPSCs necessary for cell-based therapies and drug development.

## ACKNOWLEDGMENTS

We acknowledge support from the Ministry of Education, Youth, and Sport of the Czech Republic (MSMT0021622430, LC06077), the Grant Agency of the Czech Republic (302/12/G157), the European Regional Development Fund (FNUSA-ICRC CZ.1.05/1.1.00/02.0123), and SoMoPro. The research leading to these results obtained financial contribution from the European Community within the Seventh Framework Programme (FP/2007–2013) under Grant Agreement no. 229603. The research was also financed by the South Moravian Region. We thank Majlinda Lako for hiPSC clone 4 cells, Duncan Baker for G-banding analysis, Jindřiška Hammerová for providing A375 cell samples, and Soňa Mačatová for technical assistance.

## AUTHOR CONTRIBUTIONS

M.K.: conception and design, collection and assembly of data, data analysis and interpretation, manuscript writing; K.M., A.S., and I.K.: collection and assembly of data; L.E. and S.K.: collection and assembly of data, data analysis and interpretation; A.H.: expert advice; P.D.: financial support, manuscript writing, final approval of manuscript.

## DISCLOSURE OF POTENTIAL CONFLICTS OF INTEREST

The authors indicate no potential conflicts of interest.

## REFERENCES

- Mummary CL. Cardiology: Solace for the broken-hearted? *Nature* 2005;433:585–587.
- Desbordes SC, Placantonakis DG, Socci A et al. High-throughput screening assay for the identification of compounds regulating self-renewal and differentiation in human embryonic stem cells. *Cell Stem Cell* 2008;2:602–612.
- Steiner D, Khaner H, Cohen M et al. Derivation, propagation and controlled differentiation of human embryonic stem cells in suspension. *Nat Biotechnol* 2010;28:361–364.
- Zweigerdt R, Olmer R, Singh H et al. Scalable expansion of human pluripotent stem cell in suspension culture. *Nat Protoc* 2011;6:689–700.
- Amit M, Laevsky I, Miropolsky Y et al. Dynamic suspension culture for scalable expansion of undifferentiated human pluripotent stem cells. *Nat Protoc* 2011;6:572–579.
- Olmer R, Lange A, Selzer S et al. Suspension culture of human pluripotent stem cells in controlled, stirred bioreactors. *Tissue Eng Part C Methods* 2012;18:772–784.
- Hasegawa K, Fujioka T, Nakamura Y et al. A method for the selection of human embryonic stem cell sublines with high replating efficiency after single-cell dissociation. *STEM CELLS* 2006;24:2649–2660.
- Ellerström C, Strehl R, Noaksson K et al. Facilitated expansion of human embryonic stem cells by single-cell enzymatic dissociation. *STEM CELLS* 2007;25:1690–1696.
- Bajpai R, Lesperance J, Kim M et al. Efficient propagation of single cells Accutase-dissociated human embryonic stem cells. *Mol Reprod Dev* 2008;75:818–827.
- Watanabe K, Ueno M, Kamiya D et al. A ROCK inhibitor permits survival of dissociated human embryonic stem cells. *Nat Biotechnol* 2007;25:681–686.
- Claassen DA, Desler MM, Rizzino A. ROCK inhibition enhances the recovery and growth of cryopreserved human embryonic stem cells and human induced pluripotent stem cells. *Mol Reprod Dev* 2009;76:722–732.
- Singh H, Mok P, Balakrishnan T et al. Up-scaling single cell-inoculated suspension culture of human embryonic stem cells. *Stem Cell Res* 2010;4:165–179.
- Ungrin MD, Loshi C, Nica A et al. Reproducible, ultra high-throughput formation of multicellular organization from single cell suspension-derived human embryonic stem cell aggregates. *PLoS One* 2008;13:e1565.
- Braam SR, Denning C, Matsa E et al. Feeder-free culture of human embryonic stem cells in conditioned medium for efficient genetic modification. *Nat Protoc* 2008;3:1435–1443.
- Kunova M, Matulka K, Eiselleova L et al. Development of humanized culture medium with plant-derived serum replacement for human pluripotent stem cells. *Reprod Biomed Online* 2010;21:676–686.
- Peerani R, Onishi K, Mahdavi A et al. Manipulation of signaling thresholds in “engineered stem cells niches” identifies design criteria for pluripotent stem cell screens. *PLoS One* 2009;4:e6438.
- Hough SR, Laslett AL, Grimmond SB et al. A continuum of cell states spans pluripotency and lineage commitment in human embryonic stem cells. *PLoS One* 2009;4:e7708.



- 18** Chen G, Hou Z, Gulbranson DR et al. Actin-myosin contractility is responsible for the reduced viability of dissociated human embryonic stem cells. *Cell Stem Cell* 2010;7:240–248.
- 19** Tang C, Lee AS, Volkmer JP et al. An antibody against SSEA-5 glycan on human pluripotent stem cells enables removal of teratoma-forming cells. *Nat Biotechnol* 2011;29:829–834.
- 20** Pomper MG, Hammond H, Yu X et al. Serial imaging of human embryonic stem-cell engraftment and teratoma formation in live mouse models. *Cell Res* 2009;19:370–379.
- 21** Ardehali R, Inlay MA, Ali SR et al. Overexpression of BCL2 enhances survival of human embryonic stem cells during stress and obviates the requirement for serum factors. *Proc Natl Acad Sci USA* 2011;108:3282–3287.
- 22** Amps K, Andrews PW, Anyfantis G et al. Screening ethnically diverse human embryonic stem cells identifies a chromosome 20 minimal amplicon conferring growth advantage. *Nat Biotechnol* 2011;29:1132–1144.
- 23** Bai H, Chen K, Gao YX et al. Bcl-xL enhances single-cell survival and expansion of human embryonic stem cells without affecting self-renewal. *Stem Cell Res* 2012;8:26–37.
- 24** Blum B, Bar-Nur O, Golan-Lev T et al. The anti-apoptotic gene survivin contributes to teratoma formation by human embryonic stem cells. *Nat Biotechnol* 2009;27:281–287.
- 25** Amit M, Carpenter MK, Inokuma MS et al. Clonally derived human embryonic stem cell lines remain pluripotency and proliferative potential for prolonged periods of culture. *Dev Biol* 2000;227:271–278.
- 26** Ohgushi M, Matsumura M, Eiraku M et al. Molecular pathway and cell state responsible for dissociation-induced apoptosis in human pluripotent stem cells. *Cell Stem Cell* 2010;7:225–239.
- 27** Li L, Wang BH, Wang S et al. Individual cell movement, asymmetric colony expansion, rho-associated kinase, and E-cadherin impact the clonogenicity of human embryonic stem cells. *Biophys J* 2010;98:2242–2251.
- 28** Närvä E, Autio R, Rahkonen N et al. High-resolution DNA analysis of human embryonic stem cell lines reveals culture-induced copy number changes and loss of heterozygosity. *Nat Biotechnol* 2010;28:371–377.
- 29** Tonge PD, Shigeta M, Schroeder T et al. Functionally defined substrates within the human embryonic stem cell compartment. *Stem Cell Res* 2011;7:145–153.
- 30** Enver T, Soneji S, Joshi C et al. Cellular differentiation hierarchies in normal and culture-adapted human embryonic stem cells. *Hum Mol Genet* 2005;14:3129–3140.
- 31** Stewart MH, Bossé M, Chadwick K et al. Clonal isolation of hESCs reveals heterogeneity within the pluripotent stem cell compartment. *Nat Methods* 2006;3:807–815.
- 32** Song Y, Withers DA, Hakomori S. Globoside-dependent adhesion of human embryonal carcinoma cells, based on carbohydrate-carbohydrate interaction, initiates signal transduction and induces enhanced activity of transcription factors AP1 and CREB. *J Biol Chem* 1998;273:2517–2525.
- 33** Xu Y, Zhu X, Hahm HS et al. Revealing a core signaling regulatory mechanism for pluripotent stem cell survival and self-renewal by small molecules. *Proc Natl Acad Sci USA* 2010;107:8129–8134.
- 34** Werbowetski-Ogilvie TE, Bossé M, Stewart M et al. Characterization of human embryonic stem cells with features of neoplastic progression. *Nat Biotechnol* 2009;27:91–97.
- 35** Rodin S, Domogatskaya A, Ström S et al. Long-term self-renewal of human pluripotent stem cells on human recombinant laminin-511. *Nat Biotechnol* 2010;28:611–615.



See [www.StemCellsTM.com](http://www.StemCellsTM.com) for supporting information available online.